

Interference Modelling for the Simulation of IEEE 802.11 Infrared Local Area Networks^{*}

Rui T. Valadas

Dept. of Electronics and Telecommunications,
University of Aveiro, 3810 Aveiro, PORTUGAL

Abstract

This paper proposes a model for the IEEE 802.11 infrared physical layer that includes the effect of multi-user interference through a detailed consideration of the modulation and detection techniques. The model was designed to be integrated into a discrete-event simulator of medium access protocols and allows the calculation of the frame error rate without any constraints on the length of the captured and interfering packets and on the joint distribution of the interference. With the purpose of studying the impact of the interference in the medium access protocol, the model was integrated into the discrete-event simulator RMACSIM, which was initially developed to study the performance of the IEEE 802.11 medium access mechanisms with a radio physical layer. Several simulation studies on the efficiency of the immediate priority acknowledgement and reservation mechanisms embedded in the IEEE 802.11 protocol are presented.

1. Introduction

Wireless local area networks (WLANs) will be deployed without any previous frequency or coding plan. This opens the possibility of having several collocated networks operating on the same channel. In these environments, the *multi-user interference* (occurrence of multiple simultaneous transmissions on the channel) will be one of the major factors degrading the system performance.

Infrared WLANs [3,4,6] have better resilience to interference than radio WLANs given that infrared radiation can not penetrate opaque obstacles, thus providing for a natural spatial isolation between cells. However, due to the relatively short ranges of infrared cells, multiple cells will be frequently required to cover large areas (typically exceeding 100 m²) such as conference rooms, exhibition halls and factories. In these environments infrared WLANs will be severely affected by interference.

^{*} The IEEE 802.11 standard is yet to be approved by the 802.11 group

The IEEE 802.11 group has developed a specification for WLANs, with a MAC sub-layer common to several PHY layers, including radio and infrared [5]. The medium access mechanism is based on a type of CSMA (Carrier Sense Multiple Access Protocol) protocol. With this protocol the interference can be provoked by *hidden stations*, i.e., stations that are unable to sense the activity on the medium due the transmissions of other stations [12].

Interference does not imply failure to receive a packet: the packets that compete at a receiver can have very different powers and a stronger packet can eventually be received with success. Packet reception can be viewed as a two step process: first the receiver has to synchronise with the packet header; second the information bits have to be decoded. In the presence of interference, the receiver may synchronise by one of the competing packets. This phenomenon is called *capture* [1,2,8]. The captured packet may eventually be successfully decoded.

Interference modelling is usually done by assuming that the interference can be approximated as Gaussian noise [1,9]. The Gaussian approximation is only valid for a large number of identically distributed interfering signals. These conditions may not be found in practice. This paper addresses the multi-user interference problem in IEEE 802.11 infrared WLANs by resorting to simulation techniques. The use of simulation allows a more realistic model of the interference to be implemented. In section 2 we present a global model for the IEEE 802.11 infrared physical layer, that includes the interference effect through a detailed consideration of the modulation and detection techniques. The model was developed to be integrated in the discrete-event simulator RFMACSIM [10], which was initially designed to study the IEEE 802.11 medium access mechanisms with a radio physical layer. The main features of the RFMACSIM simulator are introduced in section 3. In section 4 we present results on the error rate, with and without interference. In section 5 we present and discuss several simulation studies on the efficiency of the IEEE 802.11 medium access mechanisms. Finally, in section 6 we present our conclusions.

2. Infrared physical layer model

The infrared physical layer model was developed to be integrated into a discrete-event simulator of medium access protocols. It requires that the simulator, at each receiving station, (i) selects the captured packet when reception starts and (ii) computes the powers of the captured and interfering signals whenever a station abandons or enters the medium.

PROPAGATION: Propagation of the ambient noise is isotropic. Propagation of the infrared signal is through a single reflection (on the ceiling of a room), the emitter is Lambertian and the receiver has a full field-of-view. Emitter and receiver are located in a plane parallel to the ceiling, at an height of 3 meters. Under these conditions, the optical power received by a station is $P_R = P_E \rho A_R L_p$, where P_E is the emitted optical power, ρ is the reflection coefficient of the ceiling, A_R is the receiver active area and L_p the propagation losses. The losses can be approximated by [13]

$$L_p = \begin{cases} 88.3199 - 11.4115d + 11.4177d^2 - 1.05732d^3 + \\ 0.18581d^4 + 4.44805 \times 10^{-6}d^5 - 8.75391 \times 10^{-7}d^6, & d \leq 39.7 \\ -37552.2 + 0.171925d^4, & 39.7 < d \leq 100 \end{cases}$$

where d is the emitter - receiver distance (in meters). The exact expression for the propagation losses requires the numerical calculation of a double integral. The polynomial approximation provides a more efficient (though less flexible) model for simulation purposes.

MODULATION and DETECTION: Transmission is based on Pulse Position Modulation (PPM). In PPM, a word with k bits is encoded into one of the $L = 2^k$ positions of PPM symbol, where a pulse is transmitted. Detection is non-optimum and based on a threshold detector. The detector samples all L positions of a symbol and compares each sample with a detection threshold. A symbol error can occur (i) if the sample does not exceed the threshold in the position of the transmitted pulse or (ii) if the sample does exceed the threshold in the position of the transmitted pulse and also in at least one more position. Thus, the symbol error rate (SER), in the absence of interference from other stations, is given by

$$\begin{aligned} P_{es} &= 1 - \Pr \{n + s \geq V_T\} \Pr \{n \leq V_T\}^{L-1} \\ &= 1 - \left[1 - Q\left(\frac{s - V_T}{\sigma}\right) \right] \left[1 - Q\left(\frac{V_T}{\sigma}\right) \right]^{L-1} \end{aligned}$$

where V_T represents the detection threshold amplitude, s and n the signal and noise samples, and σ the rms noise. The signal sample is $s = RP_R$, where R is the responsivity of the photodetector. The detection threshold is adaptive with amplitude $V_T = s/2$. The ambient noise is stationary with variance $\sigma^2 = 2qRP_NB$, where P_N is the noise power and B the noise equivalent bandwidth of the receiver. The noise current is $I_N = RP_N$. The receiver transfer function formats a rectangular pulse with duration T into a raised-cosine pulse (100% roll-off). In this case $B = 0.564/T$. The detector model could have considered

optimal detection. Again this would require the numerical calculation of a double integral which could result in a less efficient implementation.

CONNECTIVITY: There is connectivity between two stations if the received optical power exceeds the receiver sensitivity, defined as the minimum optical power for a symbol error rate of 10^{-9} , assuming a noise power of -10 dBm. Resulting from the propagation model defined previously the connectivity zone is circular and can be characterised by its radius.

CARRIER SENSE: A receiving station can sense a transmitting station if the received optical power exceeds the carrier sense threshold.

INTERFERENCE: We assume that stations start their transmissions synchronously with the PPM symbol. The reception of a captured packet can be affected in non-overlapping time intervals by different sets of interfering pulses. These intervals will be denoted by *interference periods*. A new interference period is started whenever a station enters or abandons the medium during the reception of a captured packet. For the purpose of calculating the frame error rate (FER) the captured packet can be successively decomposed into interference periods, symbols and positions, as illustrated in Figure 1. The frame error rate for a captured packet with Z interference periods is

$$P_{ef} = 1 - \prod_{z=1}^Z (1 - P_z)^{l_z}$$

where P_z and l_z represent the symbol error rate and the number of symbols of the z -th interference period, respectively.

In a given interference period, each symbol is affected by the same set of interfering pulse amplitudes; only the position of the interfering pulses can vary from symbol to symbol. An interfering pulse is equally likely to hit any of the L positions of the symbol. It can hit the position of the captured pulse with probability $1/L$ or any of the remaining $L-1$ positions with probability $(L-1)/L$. In the first case it enhances the captured pulse. In the second case it may contribute to a symbol error. We will denote the position where the captured pulse was transmitted by *signal position* and the remaining positions by *noise positions*.

Let the set of interfering pulses that affect the symbol (of the z -th interference period) be $\mathbf{S} = \{s_1, s_2, \dots, s_i\}$ (s_k is the amplitude of the k -th pulse) and its indexing set be $\mathbf{I} = \{1, 2, \dots, i\}$. There are L^i equally likely patterns of i interfering pulses in L positions.

For example, assuming two interfering pulses, $\mathbf{I} = \{1,2\}$, and 3-PPM symbols, with positions p_1 to p_3 , the set of nine equally likely interference patterns is as represented in Table 1.

Each interference pattern determines a (conditioned) symbol error rate, P_{z_v} . The (unconditioned) symbol error rate can be obtained by averaging over all interference patterns:

$$P_z = \frac{\sum_{v=1}^{L^i} P_{z_v}}{L^i}$$

Table 1 shows several interference patterns which result in the same conditioned symbol error rate. Assuming that p_1 is the signal position it is clear that patterns d_2 and d_3 , d_4 and d_7 , d_5 and d_9 and also d_6 and d_8 all have the same conditioned symbol error rate. The number of non-distinct interference patterns can be relatively high. This motivates the investigation of an algorithm to isolate the interference patterns that have a distinct conditioned symbol error rate.

SYMBOL ERROR RATE ALGORITHM: Let \mathbf{N} denote the set of interference patterns that have a distinct symbol error rate. To construct \mathbf{N} , we first list, in the auxiliary set \mathbf{M} , all ordered 2-tuples with the first element being a set of interfering pulses hitting the signal position, denoted by \mathbf{I}_0 , and the second element being a set of interfering pulses hitting the noise positions as a whole, denoted by \mathbf{I}_n . Clearly in each 2-tuple $\mathbf{I}_0 \cup \mathbf{I}_n = \mathbf{I}$. Second, we further expand each set \mathbf{I}_n in ordered p -tuples with each element being a set of interfering pulses hitting a particular noise position, denoted by \mathbf{I}_1 to \mathbf{I}_p .

In the signal position any pattern corresponding to a subset of \mathbf{I} has a distinct symbol error rate. Thus, $\mathbf{M} = \{(\mathbf{I}_0, \mathbf{I}_n): \mathbf{I}_0 \subseteq \mathbf{I}, \mathbf{I}_n = \overline{\mathbf{I}_0}\}$ where $\overline{\mathbf{I}_0}$ represents the complement of \mathbf{I}_0 in \mathbf{I} . Taking the example of Table 1, $\mathbf{M} = \{(\{1,2\}, \emptyset), (\{1\}, \{2\}), (\{2\}, \{1\}), (\emptyset, \{1,2\})\}$. For each \mathbf{I}_n the interference patterns that have a distinct conditioned symbol error rate correspond to the *set partitions* [7] of \mathbf{I}_n (with the restriction that the number of partitions should be no greater than the total number of noise positions $L-1$). Thus,

$$\mathbf{N} = \{(\mathbf{I}_0, \mathbf{I}_1, \dots, \mathbf{I}_p): \mathbf{I}_0 \subseteq \mathbf{I}, (\mathbf{I}_1, \dots, \mathbf{I}_p) \text{ is a set partition of } \overline{\mathbf{I}_0}, p = L-1\}$$

We now define a one-to-one correspondence between each $(p+1)$ -tuple of \mathbf{N} and a $(p+1)$ -tuple $\mathbf{v} = (v_0, v_1, \dots, v_p)$, with v_k representing the total interfering amplitude in the k -th position of the symbol. These vectors are grouped in set \mathbf{V} defined as

$$\mathbf{V} = \left\{ (v_0, v_1, \dots, v_p) : v_i = \sum_{j \in \mathbf{I}_i} s_j, (\mathbf{I}_0, \mathbf{I}_1, \dots, \mathbf{I}_p) \in \mathbf{N} \right\}$$

Element v_0 represents the interfering amplitude in the signal position and the remaining elements, v_1 to v_p , represent the interfering amplitude in each of p noise positions. Since some noise positions may not be affected by interfering pulses it follows that $p = L-1$. The symbol error rate conditioned on the interference pattern is then given by:

$$\begin{aligned} P_{z_v} &= 1 - \Pr\{n + s + v_0 \geq V_T\} \prod_{i=1}^p \Pr\{n + v_i \leq V_T\} (\Pr\{n \leq V_T\})^{L-1-p} \\ &= 1 - \left[1 - Q\left(\frac{s + v_0 - V_T}{\sigma}\right) \right] \prod_{i=1}^p Q\left(\frac{v_i - V_T}{\sigma}\right) \left[1 - Q\left(\frac{V_T}{\sigma}\right) \right]^{L-1-p} \end{aligned}$$

The number of non-distinct interference patterns that is represented by a particular $(p+1)$ -tuple from \mathbf{N} is given by the ordered arrangements without repetition of the p elements of \mathbf{I}_n in the $L-1$ noise positions:

$$a_v = (L-1)(L-2) \dots (L-p) = \prod_{i=1}^p (L-i)$$

Finally, the (unconditioned) symbol error rate of the z -th interfering period is

$$P_z = \sum_{v \in \mathbf{V}} \frac{a_v}{L^i} P_{z_v}$$

ALGORITHM EFFICIENCY: The number of elements in \mathbf{V} (or in \mathbf{N}) is [13]

$$|\mathbf{N}| = \sum_{k=0}^i \binom{i}{k} \sum_{l=1}^{L-1} S(i-k, l)$$

where $S(n, m)$ is the Stirling number of the second kind, which describes the number of set partitions of a set with n elements into m blocks. In Figure 2 we represent the required number of calculations of the conditioned symbol error rate with the algorithm ($|\mathbf{N}|$) and without the algorithm (L^i), as a function of the number of interfering pulses, for 2-PPM, 4-PPM and 16-PPM. It can be seen that the number of calculations increases rapidly with the number of interfering pulses and with the number of positions per symbol. For $L = 2$ the number of calculations is approximately the same with or without algorithm. For $L = 4$ or $L = 16$ the gains in terms of computational efficiency which can be achieved by using the algorithm can be quite significant.

DECISION: The captured packet is received correctly if a Bernoulli trial based on the frame error rate is successful.

3. The RFMACSIM

The RFMACSIM (RF MAC SIMULATOR) is a discrete-event simulator which was designed to study the medium access protocols under consideration by the IEEE 802.11 group [10,11]. It included initially a model of a radio physical layer. It was subsequently modified to include the model of the infrared physical layer described in the previous section. In this section we present the main features of RFMACSIM.

MEDIUM ACCESS PROTOCOL: RFMACSIM implements the basic medium access mechanisms of the upcoming IEEE 802.11 standard, which is based on a CSMA/CA protocol (Carrier Sense Multiple Access with Collision Avoidance). In CSMA/CA a station with a packet ready to send starts by sensing the channel (Carrier Sense). If sensed idle for a period longer than an Inter-Frame Spacing (denoted by DIFS) the station transmits immediately. If sensed busy the station defers until the channel is sensed idle for a period longer than DIFS and then executes a truncated binary random backoff algorithm (Collision Avoidance). The algorithm imposes a random delay of an integer number of time intervals, called *slots*, before each retransmission attempt; the maximum delay in a retransmission attempt is called the *contention window*; the delay (in slots) before the n -th retransmission attempt is defined by a variable r uniformly distributed in the interval $0 = r < 2^{k-1}(CW_{min}+1)$, where $k = \min(n, 1 + \log_2[(CW_{max}+1)/(CW_{min}+1)])$ and CW_{max} and CW_{min} represent the maximum and minimum values of the contention window, respectively. The CSMA/CA protocol is further enhanced with immediate priority acknowledgement and reservation mechanisms. The *immediate priority acknowledgement* mechanism requires the destination station to acknowledge any directed valid DATA packet through an ACK mini-packet directed to the source station. In order to avoid contention when sending the ACK, the destination station uses an Inter-Frame Spacing shorter than DIFS (denoted by SIFS). The immediate priority acknowledgement mechanism can not be used with multicast and broadcast packets. The *reservation* mechanism is based on the exchange of broadcast mini-packets RTS (Request-To-Send) and CTS (Clear-To-Send) between the source and destination stations prior to sending the DATA packet. These mini-packets indicate the duration of the transaction from end of RTS (or CTS) to end of ACK. Based on the duration information broadcasted by RTS and CTS, all stations maintain a timer, the Network Allocation Vector (NAV), that indicates the remaining time for the channel to become idle. Any

station that hears a RTS or CTS mini-packet must update its NAV. In this way, stations that are hidden from the source station or the destination station (that cannot hear the RTS but hear the CTS or vice-versa) are prevented to interfere with the DATA packet.

TRAFFIC GENERATION: Packets are generated irrespective of the state of the channel and of the stations. Each station has a buffer with size for queuing Q packets. A transmission attempt is only initiated when a packet abandons the buffer. Therefore, the service position is exterior to the buffer. Generated packets are assigned to source stations according to an uniform distribution over the set of all stations. However, if the buffer of the source station is found full the packet is rejected. The destination station is also selected uniformly but only over the set of stations that have connectivity with the source station. The simulator has a resolution of $1 \mu\text{s}$. The arrival rate is geometrically distributed with average $p = R_b g / \bar{L}$ packets/ μs , where \bar{L} , R_b and g are user-defined parameters (with the restriction $p = 1$) representing the average length of DATA packets (including *overhead*), the channel bit rate and the (normalised) offered load, respectively.

SPATIAL DISTRIBUTION: Stations are spatially distributed in a rectangular grid. Each station occupies a rectangular cell with user-defined dimensions.

CAPTURE: In the presence of interference the captured packet is selected according to the following rules: (i) DATA and ACK are directed packets; they can only be selected as captured in its destination stations and are always selected as interfering in any other stations. (ii) RTS and CTS are broadcast packets; they can be selected as captured in any station. (iii) If two or more competing packets arrive simultaneously at an idle receiver, the stronger packet (highest signal) will be selected as captured. (iv) However, if a stronger packet arrives at a receiver that is already receiving a weaker packet, the stronger packet will always be considered as interfering.

PERFORMANCE METRICS: Recall that if the buffer of a station is found full the packet offered for transmission is immediately rejected. Thus we distinguish between offered packets (by the generator) and accepted packets (by a source station). Completed packets are packets that are received successfully. Define *acceptance rate* as the ratio of the accepted blocks to offered blocks and *completion rate* as the ratio of completed blocks to accepted blocks. Then,

$$\text{throughput} = g \times (\text{acceptance rate}) \times (\text{completion rate})$$

4. Symbol and Frame Error Rate

We analyse in this section the symbol and frame error rate. The parameters of the infrared physical layer follow the IEEE 802.11 specification: data rate: 1 Mbps; modulation scheme: 16-PPM; average emitted power: $P_E = 125$ mW; photodiode responsivity: $R = 0.6$; receiver active area: $A_r = 1$ cm²; ceiling reflection coefficient: $\rho = 0.7$; noise power at the receiver: $P_N = -10$ dBm. Under these conditions the noise current is 0.06 mA, the receiver sensitivity -50.6 dBm and the connectivity radius 8.12 meters.

We start by considering the case of no interfering stations. In Figure 3 we represent the SER and the FER (packets with 64 and 1046 octets) as a function of the emitter - receiver distance, for ambient noise currents of $I_N = 0.6, 0.06$ and 0.006 mA. In all cases it can be seen that the error rate varies abruptly between 0 and 1. Also the distance where the transition takes place decreases as the noise current increases. The transition region is higher in the case of the SER and lower in the case of the FER with 1046 octets. For example, in the case of the FER with 1046 octets and a noise current of $I_N = 0.6$ mA, the FER is 0.1 for an emitter - receiver distance of 6.05 meters and is 0.9 for a distance of 6.48 meters. Thus, the FER varied from 0.1 to 0.9 with a variation of the emitter - receiver distance of only 43 cm! Let Δ_d denote the width of the transition region, defined as the difference between the distance where the FER is 0.1 and the distance where the FER is 0.9. In Table 2 we list the values of Δ_d that correspond to the cases in Figure 3.

We analyse now the SER with a single interfering station. In Figure 4 we represent the SER as a function of the interferer - receiver distance, for emitter - receiver distances of 8, 9, 10, 11, 11.5 and 12 meters. An ambient noise current of $I_N = 0.06$ mA is assumed. For relatively long interferer - receiver distances the SER maintains a value approximately constant, which corresponds to the SER without interference; the SER varies abruptly as the interfering station approaches the receiver; for relatively short interferer - receiver distances the SER maintains a value between 0.9 and 1; the width of the transition region is lower for shorter emitter - receiver distances. These results illustrate that the interference can drastically affect the connectivity between two stations.

5. Simulation Studies

In this section we present simulation studies on the efficiency of the immediate priority acknowledgement and reservation mechanisms. The following parameters of the medium access protocol were considered: buffer size, $Q = 0$; slot duration: 50 μ s; minimum contention window: $CW_{min} = 31$ slots; maximum contention window: $CW_{max} = 255$ slots; retry limit: 16 attempts; SIFS duration: 28 μ s; DIFS duration: 128 μ s; DATA length:

1046 octets; ACK length: 32 octets; RTS length: 32 octets; CTS length: 26 octets. The parameters of the physical layer are as considered in previous section. In general, the simulated time was 200 seconds and simulations were run 10 times. The curves in the following sections include error bars showing the 95% confidence intervals.

5.1 Immediate Priority Acknowledgement

In section 4 we have seen that the error probability (both symbol and frame) varies rapidly between 0 and 1 with the emitter - receiver distance. To study the use of immediate priority acknowledgement we replicated the conditions of section 4, considered in the analysis of the symbol and frame error rate without interference. We assumed a configuration of 3×3 stations; the receiver sensitivity was adjusted to assure that each station in the network could only transmit to the immediately adjacent stations placed at the nearest distance. No diagonal transmissions were possible and, therefore, there was only one distance available for any communication. We will refer to this distance as the emitter - receiver distance. The carrier sense sensitivity was made arbitrarily high to assure that there were no simultaneous transmissions. The traffic load was made small ($g = 0.2$) and the buffer capacity was fixed at $Q = 5$, with the purpose of avoiding exceeding the maximum number of allowed retransmission attempts, thus keeping the acceptance rate near 1.

In Figure 5 we compare the completion rate of the protocols CSMA/CA and CSMA/CA + ACK, as a function of the emitter - receiver distance, assuming packets with 1046 octets and a noise current of $I_N = 0.06$ mA. In the case of CSMA/CA it can be seen that the completion rate is 0.5 for a distance of 9.3 meters, 0.9 for a distance of 9.1 meters and 0.1 for a distance of 9.6 meters. These values are in complete agreement with the FER values obtained in previous section. In the case of CSMA/CA + ACK, the completion rate maintains a value of 1 up to emitter - receiver distances slightly higher. For example, for a distance of 9.3 meters the completion rate is still 0.99. This is due to the possibility of retransmitting erroneously received packets introduced by the immediate priority acknowledgement mechanism. However, as in the case of CSMA/CA the completion rate varies rapidly with the emitter - receiver distance. According to Figure 5, the immediate priority acknowledgement mechanism is only advantageous for a very short range of distances: between 9 and 9.5 meters. This case study clearly illustrates that the immediate priority acknowledgement mechanism is not very effective in combating the (stationary) ambient noise.

5.2 Reservation with RTS/CTS

The reservation mechanism with RTS and CTS mini-packets can help in reducing the effect of hidden stations. RTS avoids interference provoked by stations with connectivity with the source station and the CTS avoids interference provoked by stations with connectivity with the destination station. To study this problem we considered a configuration of 4×4 stations with 7 meters spacing. In this configuration, a station placed in the network centre has only four stations in its carrier sense range. Therefore, there is a total of twelve hidden stations. The use of RTS/CTS allows a reduction in the number of hidden stations to 8 or 9, depending whether the transmission is to the interior or exterior of the network. In Figure 6 we compare the throughput achieved by the protocols CSMA/CA and RTS/CTS + CSMA/CA, for two distinct buffer sizes: $Q = 0$ e $Q = 5$. It can be seen that the protocol with RTS/CTS has always a better performance. We can then conclude that, under these conditions, the reservation mechanism is efficient in combating the interference problem.

With RTS/CTS the throughput increases with the buffer size; without RTS/CTS the throughput is initially better with $Q = 5$ but, for high traffic loads, tends to a value lower than the one obtained with $Q = 0$. To study this behaviour we start by analysing the throughput at a traffic load of $g = 2$. In Table 3 we list the values of the acceptance and completion rates. It can be seen that the acceptance rate increases considerably with the buffer capacity. However, the completion rate decreases. This is caused by the increase in the average number of packets transmitted in the channel, leading to a higher percentage of erroneous packets due to interference. We note that the interference can provoke the simultaneous destruction of several packets. In any case, for this offered load the balance between the acceptance and the completion rates results in a higher throughput with $Q = 5$. However, the effect of decreasing the completion rate tends to increase with the offered load. For an offered load of $g = 4$, the CSMA/CA has completion rates of 39.9% ($Q = 0$) and 26.5% ($Q = 5$) and acceptance rates of 64.2% ($Q = 0$) and 93.4% ($Q = 5$), resulting in a lower throughput with $Q = 5$. This effect is not seen in the protocol with RTS/CTS due to the protection against interference that the reservation mechanism provides.

6. Conclusions

We have proposed a model for the IEEE 802.11 infrared physical layer that includes the effect of interference through a detailed consideration of the modulation and detection techniques. The model was designed to be integrated into a discrete-event simulator of

medium access protocols and allows the calculation of the frame error rate without any constraints on the length of the captured and interfering packets and on the joint distribution of the interference. With the purpose of studying the impact of the interference in the medium access protocol, the model was integrated into the discrete-event simulator RFMACSIM, which was initially developed to study the performance of the IEEE 802.11 medium access protocol with a radio physical layer. Several simulation studies on the efficiency of the immediate priority acknowledgement and reservation mechanisms embedded in the IEEE 802.11 protocol are presented. We have concluded that the immediate priority acknowledgement mechanism is not efficient in combating the stationary noise provoked by ambient light and that the reservation mechanism, based on the RTS/CTS protocol, can contribute significantly to improve performance in the presence of hidden stations. However, a general statement regarding the efficiency of the reservation mechanism requires more simulation studies, covering other medium and protocol parameters.

References

- [1] - K. C. Chen, "Capture In Multiple Access Lightwave Networks Employing Direct Detect Modulations", Proceedings of the IEEE GLOBECOM'92, pp. 1344 - 1348.
- [2] - I. Cidon, H. Kodesh, M. Sidi, "Erasure, Capture, and Random Level Selection in Multi-Access Systems", IEEE Transactions on Communications, vol. 36, March 1988, pp. 263-271
- [3] - F. Gfeller, U. Bapst, "Wireless In-House Data Communication via Diffuse Infrared Radiation", Proceedings of the IEEE, vol. 67, no. 11, November 1979, pp. 1474-1486.
- [4] - F. Gfeller, P. Bernasconi, W. Hirt, C. Elisii, B. Weiss, "Dynamic Cell Planning for Wireless Infrared In-House Data Transmission", Proceedings of the 1994 International Zurich Seminar on Digital Communications, Zurich, Switzerland, March 8-11, 1994.
- [5] - Project IEEE 802.11, "Wireless LAN Medium Access Control (MAC) and Physical Layer (PHY) Specifications", Draft Standard, doc. P802.11 - D2, August 1995.
- [6] - J. Kahn, J. Barry, M. Audeh, J. Carruthers, W. Krause, G. Marsh, "Non-Directed Infrared Links for High-Capacity Wireless LANs", IEEE Personal Communications Magazine, Second Quarter 1994, pp. 12-25.
- [7] - V. Krishnamurthy, "Combinatorics: theory and applications", Ellis Horwood, 1986.
- [8] - C. Lau, C. Leung, "Capture Models for Mobile Packet Radio Networks", IEEE Transactions on Communications, vol. 40, no. 5, May 1992.
- [9] - J. Linnartz, "Narrowband Land-Mobile Radio Networks", Artech House, 1993.

[10] - C. Puig, "RF MAC Simulator Documentation", RFMACSIM Version 0.32, Apple Computer, July 29, 1993.

[11] - C. Puig, "RF MAC Simulation Highlights", IEEE P802.11, document IEEE P802.11 - 94/20, IEEE 802.11 project, Wireless Access Method and Physical Layer Specification, January 1994.

[12] - F. Tobagi, L. Kleinrock, " Packet Switching in Radio Channels: Part II - The Hidden Terminal Problem in Carrier Sense Multiple-Access and the Busy-Tone Solution", IEEE Transactions on Communications, vol. COM-23, n° 12, December 1975, pp. 1417-1433.

[13] - R. Valadas, "Infrared Wireless Local Area Networks", PhD thesis (in Portuguese), University of Aveiro, Portugal, November 1995.

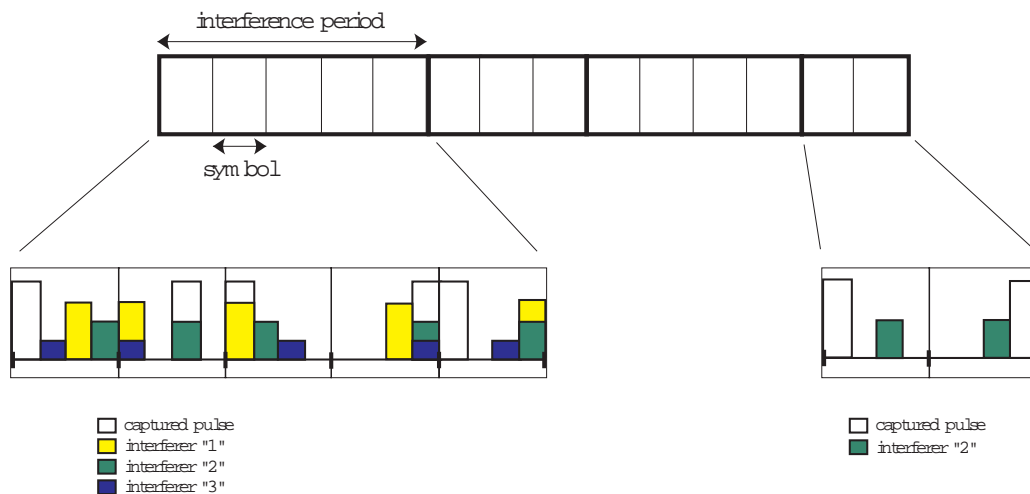


Figure 1: Decomposition of the captured packet in interference periods, symbols and positions, in a 4-PPM system.

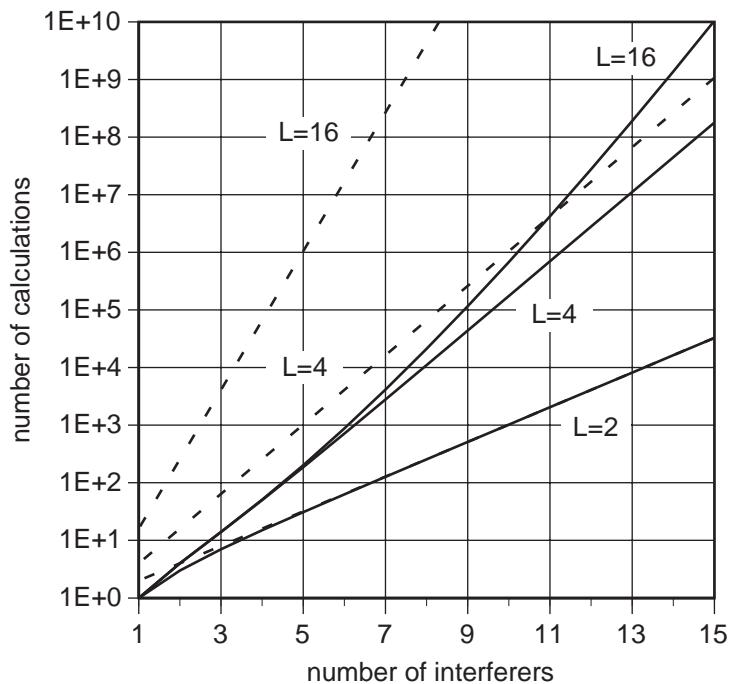


Figure 2: Number of calculations of the conditioned SER as a function of the number of interfering pulses, for 2-PPM, 4-PPM and 16-PPM, with algorithm (bold) and without algorithm (dashed).

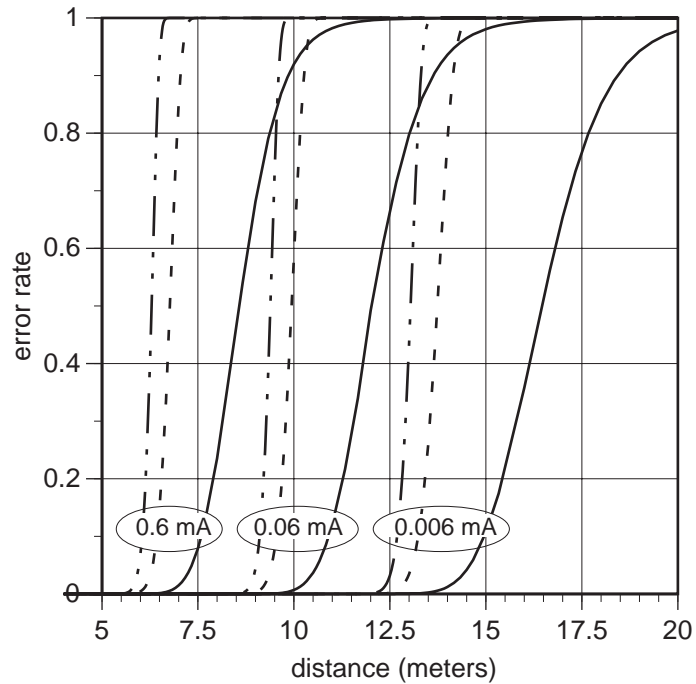


Figure 3: Symbol Error Rate (bold) and Frame Error Rate with 64 octets (dashed) and with 1046 octets (dot-dot-dash), as a function of the emitter - receiver distance, for noise currents of 0.6, 0.06 and 0.006 mA.

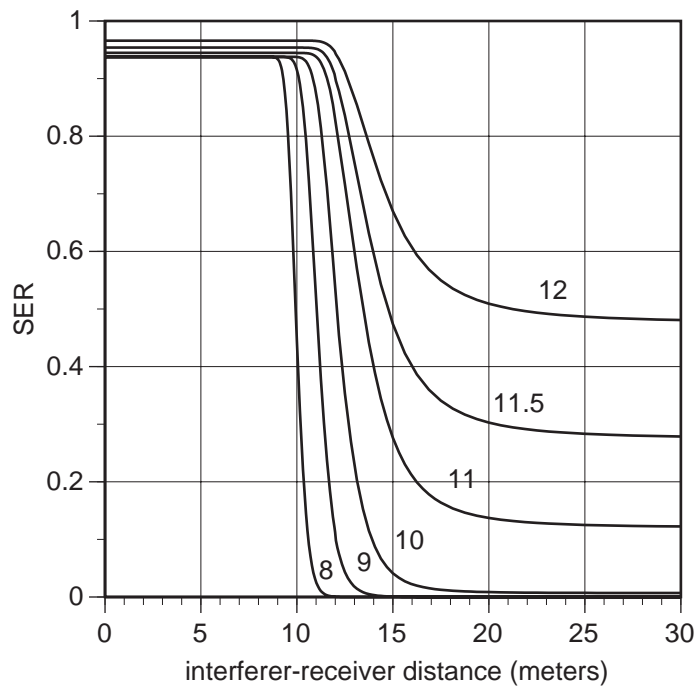


Figure 4: Frame Error Rate as function of the interferer - receiver distance, for emitter - receiver distances of 8, 9, 10, 11, 11.5 and 12 meters.

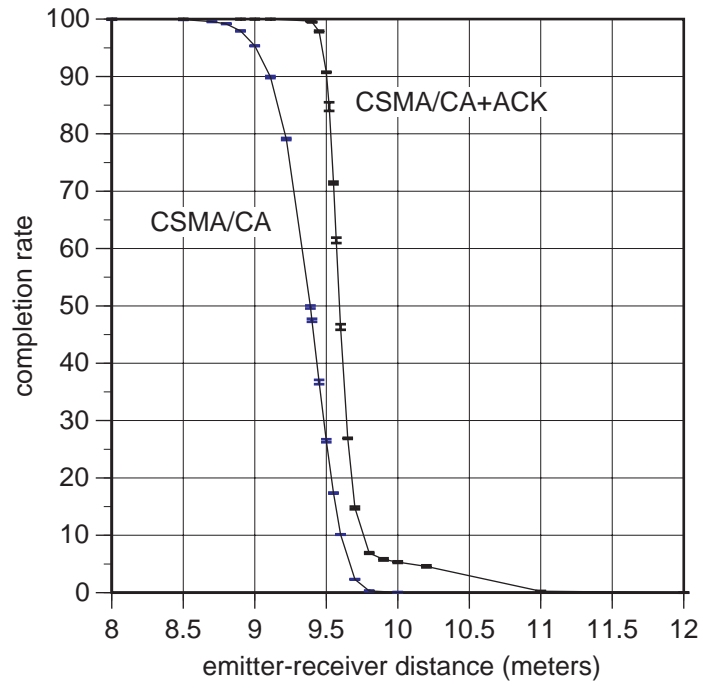


Figure 5: Completion rate as a function of the emitter - receiver distance, for a configuration of 3x3 stations.

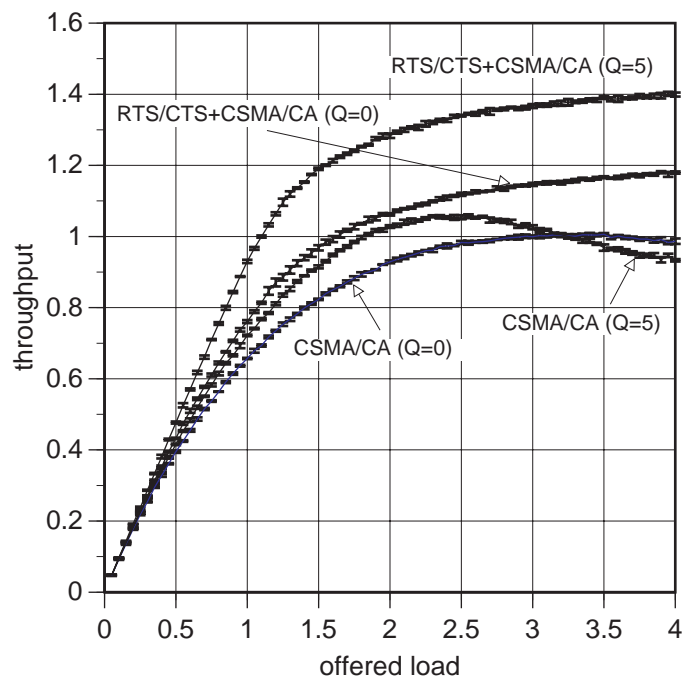


Figure 6: Throughput as a function of the offered load, for the case of the CSMA/CA protocol with and without RTS/CTS, for buffer sizes of $Q = 5$ and $Q = 0$.

	p_1	p_2	p_3
d_1	1,2		
d_2	1	2	
d_3	1		2
d_4	2	1	
d_5		1,2	
d_6		1	2
d_7	2		1
d_8		2	1
d_9			1,2

Table 1: Interference patterns of two interfering pulses, denoted by “1” and “2”, in 3-PPM symbols.

Δ_d (meters)	SER	FER (64)	FER (1046)
0.006 mA	3.47	0.90	0.62
0.06 mA	2.72	0.72	0.49
0.6 mA	2.26	0.62	0.43

Table 2: Values of Δ_d for the cases considered in Figure 3.

	Q = 0		Q = 5	
	AR	CR	AR	CR
CSMA/CA	79.4	62.0	100	54.8
RTS/CTS+CSMA/CA	59.4	95.5	86.2	79.4

Table 3: Acceptance Rate (AR) and Completion Rate (CR) for an offered load of $g = 2$.